Lattice Polytopes and Orbifolds

Matthew DeCross

October 4, 2015

1   Introduction

Recent work [1–4] in the context of *quiver gauge theories* has focused on enumeration of Abelian orbifolds of $\mathbb{C}^n$ whose toric diagrams are lattice simplices in $\mathbb{R}^{n-1}$. For example, Abelian orbifolds of $\mathbb{C}^3$ have toric diagrams that are lattice triangles with corresponding symmetry group S_3. In this work, we consider a larger set of orbifolds with geometrically interesting toric diagrams.

First, we will examine a member of a class of toric Calabi-Yau varieties which are surfaces of positive curvature, the del Pezzo surfaces. Specifically, we enumerate the orbifolds of the affine cone over the del Pezzo 3 surface (dP_3), which is described by the projective two-space $\mathbb{P}^2$ blown up at 3 generic points [5,6]. Such orbifolds have hexagonal toric diagrams with corresponding symmetry group D_6 [7]. We will show that regardless of the larger order of the symmetry group, the number of orbifolds of the dP_3 toric diagram up to $GL(2,\mathbb{Z})$ equivalence is the same as the number of inequivalent Abelian orbifolds of $\mathbb{C}^3$.

Secondly, we will enumerate orbifolds whose toric diagrams correspond to the Platonic solids. In the case of the tetrahedron, we are enumerating Abelian orbifolds of $\mathbb{C}^4$, with symmetry group corresponding to S_4. More exotic orbifolds may have toric diagrams given by the other Platonic solids: the cube, octahedron, dodecahedron, and icosahedron. Since the cube and octahedron diagrams are dual to each other, as are the dodecahedron and icosahedron, we need only additionally consider the cube and dodecahedron to enumerate orbifolds of all independent diagrams (the tetrahedron is self-dual). The relevant symmetry group for the cube is the full octahedral group, $S_4 \times \mathbb{Z}_2$, and for the dodecahedron it is the full icosahedral group, $A_5 \times \mathbb{Z}_2$.

Motivation for studying the Platonic solids comes from the ADE classification of discrete subgroups of $SU(2)$. Under the so-called McKay correspondence, there exists a bijection between the McKay graphs of the binary polyhedral groups and the simply laced affine Dynkin diagrams corresponding to the Lie algebras of A_n, D_n, and E_n [8]. Specifically the relevant correspondence is between

- A_n: binary cyclic group of order $2n$

- D_n: binary dihedral group of order $4n$

- E_6: binary tetrahedral group of order 24

- E_7: binary octahedral group of order 48

- E_8: binary icosahedral group of order 120

The ADE diagrams are interesting to study in connection with quiver gauge theories [9] because they are the unique set of quivers with only finitely many isomorphism classes of indecomposable representations. Taking the image of each group in the above correspondence under the canonical $\mathrm{Spin}(3) \to SO(3)$ double cover of the rotation group, one obtains the rotational symmetry groups D_n of the two-dimensional lattice

polygons and the groups A_4, S_4, and A_5 corresponding to the orientation-preserving symmetries of the three-dimensional Platonic solids.

This work will be organized as follows: In Section II, we will review a method of enumerating inequivalent lattice polytope toric diagrams via the symmetries of lattice points contained in the polytopes, using Burnside's lemma and the cycle index for the symmetry groups of the toric diagrams. In Section III, we review the methods of generating functions used in obtaining analytic expressions for the enumeration of inequivalent toric diagrams in any number of dimensions. Finally, in Section IV, these methods will be applied successively to the orbifolds of $\mathbb{C}^3$ and the conifold (previously computed in [1]), the dP_3 surface, and the Platonic solids.

2 Algebraic Approach to Orbifold Enumeration

2.1 Cycle Index and Burnside's Lemma

We would like to be able to count the number of independent orbifolds of an arbitrary toric diagram up to $GL(2, \mathbb{Z})$ equivalence. In [4], there was a convenient way to count the independent triangular toric diagrams using the fact that $GL(2, \mathbb{Z})$ duality is equivalent to preserving barycentric coordinates of interior and boundary lattice points. For more complicated orbifolds than lattice simplices, there is no obvious appropriate generalization of the barycentric coordinates technique and we must consider more involved algebraic methods.

A well-known theorem states that for any matrix A with integer entries there is a unique $n \times n$ matrix H with integer entries such that $H = UA$ with $U \in GL(n, \mathbb{Z})$ and H in Hermite normal form (HNF). A matrix in Hermite normal form is an upper triangular integer matrix whose superdiagonal entries are strictly smaller than the entries on the diagonal in the corresponding column.

Since toric diagrams take coordinates on integer lattices, to enumerate inequivalent toric diagrams it is thus sufficient to enumerate inequivalent HNFs. An arbitrary HNF canonically generates a sublattice of a given lattice by operating on the lattice basis by left multiplication. In this work we take a slightly different approach, where the HNF operates by left multiplication on the vertices of a given toric diagram. The linearly transformed toric diagram thus generates a sublattice via the lattice points contained in the diagram, with index $n = \det H$. For two-dimensional planar lattice polytopes, Pick's theorem tells us that the indices of these sublattices are quantized in units of $1/2$; we let n refer to the multiple of $1/2$ as opposed to the true area of the toric diagrams. In higher dimensions n will in general refer to the index of the lattice. This method is advantageous because it provides a more refined lattice than the lattice obtained by fixing the toric diagram and transforming the standard integer lattice. In dimensions greater than or equal to three, further refinements will also be necessary.

One can enumerate inequivalent sublattices of a given lattice by considering the symmetry groups of the fundamental toric diagram. The connection is provided by Burnside's lemma. First, we introduce the concept of a *cycle index* of a group [1]. Note that for any group G acting on a set of order k we can construct a homomorphism to a permutation representation, i.e. a subgroup of the symmetric group. Suppose g in the permutation representation of G consists of α_1 1-cycle, α_2 2-cycles, up to α_k k-cycles, which we may call its *cycle structure*. Then for each g we can write the expression:

$$\zeta_g(x_1, \ldots x_n) = x_1^{\alpha_1} x_2^{\alpha_2} \ldots x_k^{\alpha_k}. \tag{1}$$

Definition. The *cycle index* Z_G of a group G is obtained by averaging the ζ_g over all elements $g \in G$.

This is equivalent to:

$$Z_G = \frac{1}{|G|} \sum_\alpha c(\alpha_1, \ldots, \alpha_k) x_1^{\alpha_1} \ldots x_k^{\alpha_k}, \tag{2}$$

where $c(\alpha_1, \ldots, \alpha_k)$ denotes the number of elements of G that are permutations with the α_1 1-cycles, ..., and α_k k-cycles, and the sum is taken over each independent type of cycle structure in G.

We can use this to enumerate $GL(n, \mathbb{Z})$-inequivalent sublattices by Burnside's lemma [1]:

Lemma. *Let G be a group acting on a set X. The number $N(G)$ of orbits of G under the group action on X is given by the average size of the fixed sets under each element of G:*

$$N(G) = \frac{1}{|G|} \sum_{g \in G} |F_g|, \tag{3}$$

where F_g denotes the elements of X that are fixed by g.

The key connection is that the number of $GL(n, \mathbb{Z})$-inequivalent sublattices of index n generated by a given toric diagram with symmetry group G is equivalent to the number of orbits of G when acting on the set X_n of sublattices of index n. A given symmetry g of a toric diagram with a cycle structure $[\alpha_1 \ldots \alpha_k]$, will fix some number of sublattices $|F_g|$. We say these sublattices are invariant under the given symmetry. Note that according to the formula (2), we only need one element with each cycle structure. To be exact, we need to enumerate invariant sublattices under each conjugacy class in G.

We can thus write the total number of inequivalent sublattices of index n of a given lattice L as:

$$f^L(n) = \frac{1}{|G|} \sum_\alpha c(\alpha) f^L_{\mathbf{x}^\alpha}(n), \tag{4}$$

where $f^L_{\mathbf{x}^\alpha}(n)$ gives the number of sublattices of index N in the lattice L that are invariant under a symmetry from the conjugacy class with particular cycle structure α. The sum is thus over each conjugacy class, and $c(\alpha)$ gives the order of each conjugacy class.

The identity is in its own conjugacy class of every group; this is a special class because the sublattices symmetric under the identity are exactly the total number of sublattices at each index n. It is shown in [1] that the number of sublattices depends only on the dimension d of the lattice and is given by the formula:

$$f^{L_d}_{x_1^m}(n) = \sum_{\substack{k_0, \ldots, k_{d-1}=1 \\ k_0 k_1 \ldots k_{d-1}=n}}^n k_1 k_2^2 \ldots k_{d-1}^{d-1}, \tag{5}$$

where m corresponds to the number of elements that G acts on in its permutation representation.

In two dimensions, this is given more succinctly by the formula:

$$f^{L_2}_{x_1^m}(n) = \sum_{k|n} g^{L_2}_{x_1^m}(k), \tag{6}$$

where $g^{L_2}_{x_1^m}(k)$ denotes the number of possible 2×2 HNFs of index n and lower right entry k that generate a sublattice of L_2. Generalizations to higher dimensions are straightforward and given in [1].

3

2.2 Algorithmic Enumeration of Inequivalent Toric Diagrams

The specific algorithm for generating sublattices and enumerating inequivalent toric diagrams in two dimensions proceeds as follows. First, the toric diagram is transformed by an HNF. The integer lattice points contained in the transformed toric diagram are then enumerated. This includes points on the boundary and vertices of the transformed toric diagram. The HNF transformation is then inverted, carrying the full set of lattice data to the original toric diagram. One can then check which of the symmetries of the original toric diagram are respected by the sublattice. Repeating this procedure for all HNFs at a fixed index n, the number of invariant sublattices under each conjugacy class of the symmetry group action, corresponding to terms in the cycle index for the group, may be enumerated.

Even in two dimensions, this presents algorithmic challenges in determining which lattice points are contained in a transformed toric diagram. The method used in this work relies on the fact that any convex polygon in two dimensions can be triangulated. To determine if a lattice point is contained in a transformed toric diagram, we triangulate the diagram and compute the barycentric coordinates of the lattice point with respect to each triangle. If the barycentric coordinate components with respect to at least one of the triangles are entirely nonnegative, the lattice point is contained in the toric diagram.

There are numerous complications that arise in finding symmetric sublattices when generalizing in three dimensions and higher. Identical barycentric coordinates of lattice points of simplices generated by 3×3 Hermite normal forms are no longer sufficient to uniquely identify equivalence classes of orbifolds. In [4] it was shown that two barycentric-coordinate equivalent simplices could correspond to different orbifold actions on $\mathbb{C}^4$. The same paper introduced a method to rectify this problem. Scaling the three-dimensional simplices until their relevant lattice points included points on edges, faces, *and* the interior of the simplex was postulated to be sufficient to identify distinct orbifold actions. This method works by refinement of the lattice; by providing additional points, scaling broke some unwanted degeneracies of the sublattices. The increased complexity of searching both the larger space of 3×3 Hermite normal forms as well as the additional scaling parameter makes the computation of symmetric sublattices in the cycle index computationally intensive. In this work, a more reliable method was implemented wherein the toric diagrams were scaled until a fixed point of invariant sublattices was reached; this guarantees that further refinement of the lattice will not change the enumeration of equivalence classes.

Identifying lattice points in three dimensions also becomes more computationally challenging. In two dimensions, for lattice simplices one can merely check the sign of the barycentric coordinates of a given point with respect to the simplex to see if the point is contained in the simplex or not. For more complicated polygons in two dimensions, one can triangulate the polygon into simplices and reapply the same algorithm, as stated above. The construction for arbitrary polytopes in three dimensions is similar but computationally harder. For tetrahedra, given a test point x one can consider the set of all sub-tetrahedra with three vertices on the polytope in question and fourth given by x. If the volume of all sub-tetrahedra equals the volume of the simplex, the point x is contained in the polytope. This is slightly computationally easier than computing barycentric coordinates. More importantly, it permits ready generalization to arbitrary polytopes by triangulating the faces of the polytope and iterating this method.

3 Analytic Expressions for Orbifold Enumeration

3.1 Multiplicative Sequences and Dirichlet Convolution

The sequences corresponding to the independent terms of the cycle index often have the property of being *multiplicative*, i.e. for n, m coprime, $f(nm) = f(n)f(n)$ for a given sequence f. Multiplicative sequences

are well-studied in number theory and have many nice properties that permit semi-analytic expressions, in part due to the fact that they form a group under the *Dirichlet convolution* operation:

Definition. The *Dirichlet convolution* of two sequences g and h is the sequence f defined by

$$f(n) = (g * h)(n) = \sum_{m|n} g(m)h(\frac{n}{m}), \tag{7}$$

where the notation $m|n$ means that the sum runs over all the divisors m of n.

Semi-analytic expressions for terms in the cycle index are extremely useful because explicit algorithmic counting of terms is extremely limited by computational power. Finding semi-analytic expressions thus permits extrapolation of the limited data to arbitrarily large lattice index, allowing enumeration of orbifolds by very large finite groups.

These semi-analytic expressions for multiplicative sequences can often be built from Dirichlet convolution of simpler base sequences. To this end, define the unit, number, and square sequences:

$$u = \{1, 1, 1 \ldots\}, \tag{8}$$
$$N = \{1, 2, 3 \ldots\}, \tag{9}$$
$$N^2 = \{1, 4, 9, \ldots\}. \tag{10}$$

Inverting these base sequences is also useful for constructing semi-analytic expressions. The inverse of the unit is the *Möbius function*:

$$\mu(n) = \begin{cases} 1 & \text{if } n \text{ is the square-free product of an even number of distinct primes,} \\ -1 & \text{if } n \text{ is the square-free product of an odd number of distinct primes,} \\ 0 & \text{otherwise.} \end{cases} \tag{11}$$

and the inverse of the number sequence can be written by component as

$$N^{-1}(n) = n \cdot \mu(n). \tag{12}$$

Generically we may construct inverse sequences via the formula [1]:

$$f^{-1}(n) = -\frac{1}{f(1)} \sum_{d|n, d<n} f(\frac{n}{d}) f^{-1}(d). \tag{13}$$

Lastly, there exists a set of periodic sequences called the Dirichlet characters $\chi_{k,n}$ of modulus k and index n which are well-known to be useful in constructing multiplicative sequences. At each fixed k, the Dirichlet characters form an Abelian group of order $\varphi(k)$ where $\varphi(x)$ is Euler's totient function. Here are the Dirichlet characters $\chi_{k,n}$ up to modulo 10 from [2]. The symbol ω below denotes the sixth root of unity $\omega = \exp(i\pi/3)$. The elements given below are one full period of each infinite sequence:

$$\chi_{1,1} = u$$
$$\chi_{2,1} = \{1, 0, \ldots\}$$
$$\chi_{3,1} = \{1, 1, 0, \ldots\}$$
$$\chi_{3,2} = \{1, -1, 0, \ldots\}$$
$$\chi_{4,1} = \{1, 0, 1, 0, \ldots\}$$
$$\chi_{4,2} = \{1, 0, -1, 0, \ldots\}$$
$$\chi_{5,1} = \{1, 1, 1, 1, 0, \ldots\}$$
$$\chi_{5,2} = \{1, i, -i, -1, 0, \ldots\}$$
$$\chi_{5,3} = \{1, -1, -1, 1, 0, \ldots\}$$
$$\chi_{5,4} = \{1, -i, i, -1, 0, \ldots\}$$
$$\chi_{6,1} = \{1, 0, 0, 0, 1, 0, \ldots\}$$
$$\chi_{6,2} = \{1, 0, 0, 0, -1, 0, \ldots\}$$
$$\chi_{7,1} = \{1, 1, 1, 1, 1, 1, 0, \ldots\}$$
$$\chi_{7,2} = \{1, -\omega, \omega^2, \omega^2, -\omega, 1, 0, \ldots\}$$
$$\chi_{7,3} = \{1, \omega^2, \omega, -\omega, -\omega^2, -1, 0, \ldots\}$$
$$\chi_{7,4} = \{1, 1, -1, 1, -1, -1, 0, \ldots\}$$
$$\chi_{7,5} = \{1, -\omega, -\omega^2, \omega^2, \omega, -1, 0, \ldots\}$$
$$\chi_{7,6} = \{1, \omega^2, -\omega, \omega, \omega^2, 1, 0, \ldots\}$$

$$\chi_{8,1} = \{1, 0, 1, 0, 1, 0, 1, 0, \ldots\}$$
$$\chi_{8,2} = \{1, 0, 1, 0, -1, 0, -1, 0, \ldots\}$$
$$\chi_{8,3} = \{1, 0, -1, 0, 1, 0, -1, 0, \ldots\}$$
$$\chi_{8,4} = \{1, 0, -1, 0, -1, 0, 1, 0, \ldots\}$$
$$\chi_{9,1} = \{1, 1, 0, 1, 1, 0, 1, 1, 0, \ldots\}$$
$$\chi_{9,2} = \{1, \omega, 0, \omega^2, -\omega^2, 0, -\omega, -1, 0, \ldots\}$$
$$\chi_{9,3} = \{1, \omega^2, 0, -\omega, -\omega, 0, \omega^2, 1, 0, \ldots\}$$
$$\chi_{9,4} = \{1, -1, 0, 1, -1, 0, 1, -1, 0, \ldots\}$$
$$\chi_{9,5} = \{1, -\omega, 0, \omega^2, \omega^2, 0, -\omega, 1, 0, \ldots\}$$
$$\chi_{9,6} = \{1, -\omega^2, 0, -\omega, \omega, 0, \omega^2, -1, 0, \ldots\}$$
$$\chi_{10,1} = \{1, 0, 1, 0, 0, 0, 1, 0, 1, 0, \ldots\}$$
$$\chi_{10,2} = \{1, 0, i, 0, 0, 0, -i, 0, -1, 0, \ldots\}$$
$$\chi_{10,3} = \{1, 0, -1, 0, 0, 0, -1, 0, 1, 0, \ldots\}$$
$$\chi_{10,4} = \{1, 0, -i, 0, 0, 0, i, 0, -1, 0, \ldots\}.$$

3.2 Generating Functions and Asymptotic Distributions

Semi-analytic expressions for multiplicative sequences obtained above can be written in terms of generating functions that are either Dirichlet series or power series. These take the form:

$$F(s) = \sum_{n=1}^{\infty} \frac{f(s)}{n^s}, \qquad G(t) = \sum_{n=1}^{\infty} G(n)t^n. \tag{14}$$

The first is useful in that it lets us recover asymptotic behavior of the sequence, the second in that it provides a convenient encoding of the numerical data of the sequence.

Such generating functions are very nice to work with in the sense that they convert Dirichlet convolutions of sequences into ordinary products of functions. Namely, if $f = g * h$, the power series can be written [1]:

$$F(t) = \sum_{k=1}^{\infty} \sum_{m=1}^{\infty} g(m)h(k)t^{mk}, \tag{15}$$

and the Dirichlet series obey:

$$F(s) = G(s)H(s). \tag{16}$$

As stated, asymptotic behavior of sequences obtained from orbifold enumeration can be derived from the corresponding Dirichlet series. We quote the following theorem [1]:

Theorem. *Let $F(s)$ be a Dirichlet series with non-negative coefficients that converges for $\Re(s) > \alpha > 0$, and suppose that $F(s)$ is holomorphic in all points of the line $\Re(s) = \alpha$, except for $s = \alpha$. If for $s \to \alpha^+$, the Dirichlet series behaves as*

$$F(s) \sim A(s) + \frac{B(s)}{(s - \alpha)^{m+1}}, \tag{17}$$

where $m \in \mathbb{N}$, and both $A(s)$ and $B(s)$ are holomorphic in $s = \alpha$, then the partial sum of the coefficients is asymptotic to:

$$\sum_{n=1}^{N} a_n \sim \frac{B(\alpha)}{\alpha \, m!} N^\alpha \log^m(N). \tag{18}$$

By looking at the residues of the Dirichlet series of multiplicative sequences we may thus obtain asymptotic behavior. Furthermore, we may use *Robin's inequality* to obtain upper bounds for the growth in number of orbifolds:

$$\sigma(n) < e^\gamma n \log \log n, n \geq 5041, \tag{19}$$

where $\sigma(n)$ is the sum-of-divisors function and γ is the Euler-Mascheroni constant, which holds iff the Riemann hypothesis is true.

4   Numerical and Analytical Results

4.1   Orbifolds of $\mathbb{C}^3$

As previously stated, the orbifolds of $\mathbb{C}^3$ have toric diagrams that are lattice triangles. However, there is no triangle with true S_3 symmetry with vertices on the square integer lattice. To count sublattices invariant under various symmetries, one solution is to project triangles upwards into $\mathbb{R}^3$, where there are regular triangles on the lattice. After performing this projection, one can simply use the three-dimensional fundamental representation of the S_3 to operate on the matrix of lattice points and check to see if this matrix is invariant up to permutation under such action.

S_3 has cycle index given by:

$$Z_{S_3} = \frac{1}{6}(x_1^3 + 3x_1^1 x_2^1 + 2x_3^1), \tag{20}$$

where the action is given by permutation of the vertices of the lattice triangle. The independent elements correspond to the identity, swapping of two vertices (reflection about the midpoint of a side), and rotation of the triangle, respectively.

The results of the implementation of this algorithm for the $\mathbb{C}^3$ orbifolds are displayed below. Here we provide results out to $n = 32$ in Table 1, going beyond the published result in [1].

We also reproduce here the semi-analytic expressions for extrapolations of these sequences, from [1]:

$$f_{x_1^3}^{\triangle} = u * N, \tag{21}$$

$$f_{x_1^1 x_2^1}^{\triangle} = \{1, -1, 0, 2\} * u * u, \tag{22}$$

$$f_{x_3}^{\triangle} = \chi_{3,2} * u. \tag{23}$$

The extrapolation of the data from these semi-analytic expressions is displayed in Figure 1.

7

n	1	2	3	4	5	6	7	8	9	10	11	12	13	14	15	16
$f^{\triangle}_{x_1^3}$	1	3	4	7	6	12	8	15	13	18	12	28	14	24	24	31
$f^{\triangle}_{x_1 x_2}$	1	1	2	3	2	2	2	5	3	2	2	6	2	2	4	7
$f^{\triangle}_{x_3}$	1	0	1	1	0	0	2	0	1	0	0	1	2	0	0	1
$f^{\triangle}$	1	1	2	3	2	3	3	5	4	4	3	8	4	5	6	9

n	17	18	19	20	21	22	23	24	25	26	27	28	29	30	31	32
$f^{\triangle}_{x_1^3}$	18	39	20	42	32	36	24	60	31	42	40	56	30	72	32	63
$f^{\triangle}_{x_1 x_2}$	2	3	2	6	4	2	2	10	3	2	4	6	2	4	2	9
$f^{\triangle}_{x_3}$	0	0	2	0	2	0	0	0	1	0	1	2	0	0	2	0
$f^{\triangle}$	4	8	5	10	8	7	5	15	7	8	9	13	6	14	7	15

Table 1: Number of sublattices of index n invariant under representative symmetries from each conjugacy class of S_3, for the orbifolds of $\mathbb{C}^3$.
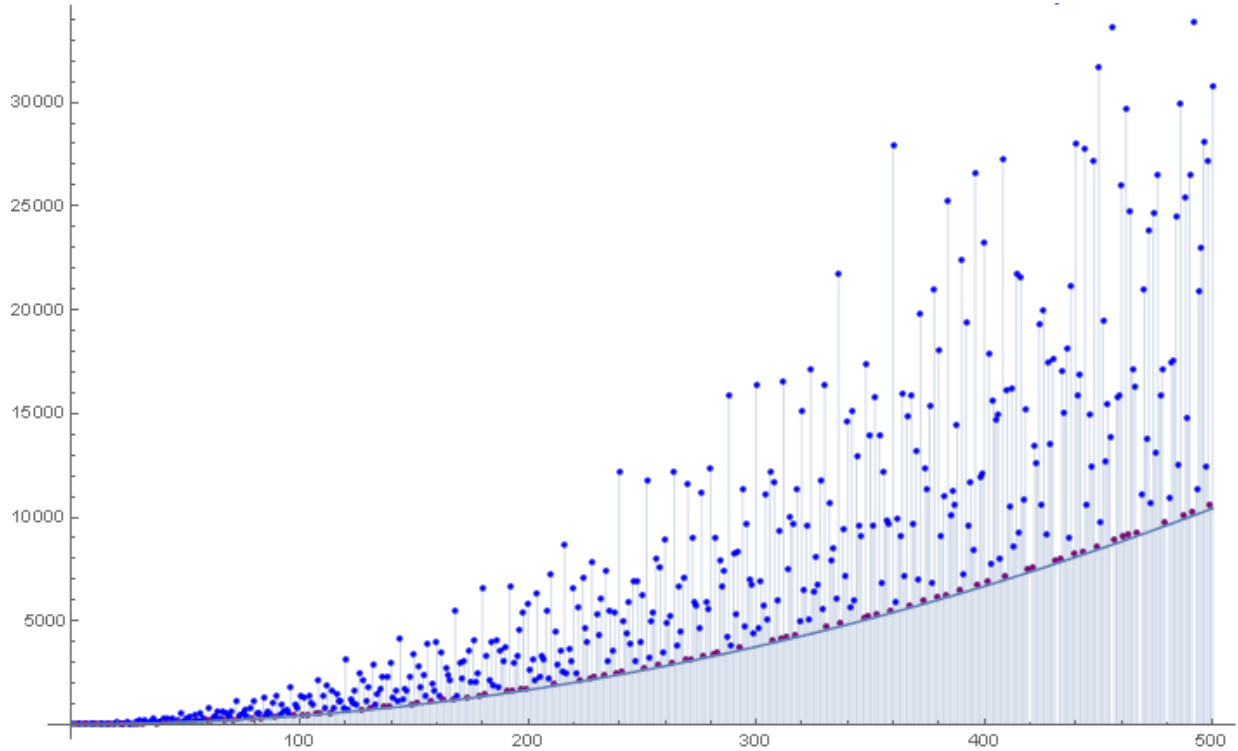

Figure 1: Scatter plot of the number of invariant sublattices of index n for the triangular lattice. Primes are given in purple. The two lines correspond to $n/6$ and $e^{\gamma} n \log \log n/6$.

Writing the Dirichlet and power series generating functions for each term in the cycle index, we find:

$$G^{\triangle}_{x_1^3} = \frac{1+t^3}{(1-t)(1-t^2)} - 1, \tag{24}$$

$$G^{\triangle}_{x_1^1 x_2^1} = \frac{1+t^3}{(1-t)(1+t^2)} - 1, \tag{25}$$

$$G^{\triangle}_{x_3^1} = \frac{(1+t)(1-t^2)}{1-t^3} - 1, \tag{26}$$

$$F^{\triangle}_{x_1^3} = \zeta(s-1), \tag{27}$$

$$F^{\triangle}_{x_1^1 x_2^1} = (1 - 2^{-s} + 2^{1-2s})\zeta(s), \tag{28}$$

$$F^{\triangle}_{x_3^1} = L(s, \chi_{3,2}). \tag{29}$$

where $L(s, \chi_{n,k})$ is the *L-function*, which is the Dirichlet series corresponding to the Dirichlet character $\chi_{n,k}$. The total Dirichlet series can thus be written:

$$F^{\triangle} = \frac{\zeta(s)}{6}\left(\zeta(s-1) + 3(1 - 2^{-s} + 2^{1-2s})\zeta(s) + 2L(s, \chi_{3,2})\right). \tag{30}$$

The rightmost pole is at $s = 2$ and is of order 1 with residue $\zeta(2)/6$. The asymptotic behavior of partial sums is thus [1]:

$$\sum_{n=1}^{N} f^{\triangle}(n) \sim \frac{\zeta(2)}{12}N^2 = \frac{\pi^2}{72}N^2, \tag{31}$$

and the growth of the sequence is thus linear. We can also write an upper bound using Robin's inequality of:

$$f^{\triangle}(n) < \frac{e^{\gamma}n\log\log n}{6}. \tag{32}$$

4.2 Orbifolds of the Conifold

The orbifolds of the conifold can be represented by square toric diagrams. The square has symmetry group D_4 with cycle index:

$$Z_{D_4} = \frac{1}{2}Z(C_4) + \frac{1}{4}(x_1^2 x_2 + x_2^2) \tag{33}$$

$$= \frac{1}{8}\sum_{d|4}\varphi(d)x_d^{4/d} + \frac{1}{4}(x_1^2 x_2 + x_2^2) \tag{34}$$

$$= \frac{1}{8}x_1^4 + \frac{1}{8}x_2^2 + \frac{1}{4}x_4^1 + \frac{1}{4}x_1^2 x_2 + \frac{1}{4}x_2^2 \tag{35}$$

$$= \frac{1}{8}x_1^4 + \frac{3}{8}x_2^2 + \frac{1}{4}x_4^1 + \frac{1}{4}x_1^2 x_2. \tag{36}$$

The group is generated by rotation x by $\pi/2$ and reflection y about a diagonal. In permutation representation, $x = (1234)$, $y = (13)$. There are five conjugacy classes that contribute to the four terms in the cycle index, given by:

$$\{1\}, \{x, x^3\}, \{x^2\}, \{y, x^2 y\}, \{xy, x^3 y\},$$

and thus representative elements in permutation representation for each conjugacy class are:

$$(1), (1234), (13)(24), (13), (12)(34).$$

Writing each term in the cycle index to correspond to the conjugacy classes, we find:

$$Z_{D_4} = \frac{1}{8}(x_1^4 + 2x_2^2 + 2x_4^1 + x_2^{2'} + 2x_1^2 x_2),$$

where we have pulled out the term $x_2^{2'}$ that corresponds to x^2, rotation by π, which is in its own conjugacy class. The representative symmetries corresponding to each conjugacy class are given above; all can be foudn by composition of rotation by $\pi/2$ with reflection about a diagonal. The resulting data is displayed in Table 2.

n	1	2	3	4	5	6	7	8	9	10	11	12	13	14	15	16
$f_{x_1^4}^{\square}$	1	3	4	7	6	12	8	15	13	18	12	28	14	24	24	31
$f_{x_1^2 x_2^1}^{\square}$	1	1	2	3	2	2	2	5	3	2	2	6	2	2	4	7
$f_{x_2^2}^{\square}$	1	3	2	5	2	6	2	7	3	6	2	10	2	6	4	9
$f_{x_2^{2'}}^{\square}$	1	3	4	7	6	12	8	15	13	18	12	28	14	24	24	31
$f_{x_4^1}^{\square}$	1	1	0	1	2	0	0	1	1	2	0	0	2	0	0	1
$f^{\square}$	1	2	2	4	3	5	3	7	5	7	4	11	5	8	8	12

Table 2: Number of sublattices of index n invariant under representative symmetries from each conjugacy class of D_4, for the orbifolds of the conifold.
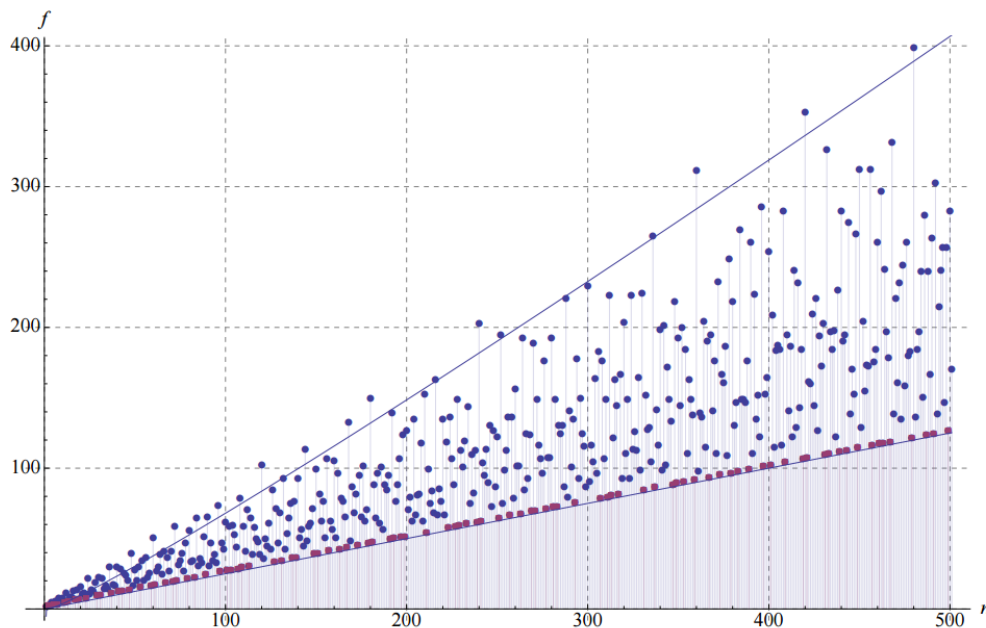

Figure 2: Scatter plot of the number of invariant sublattices of index n for the square lattice. Primes are given in purple. The two lines correspond to $n/4$ and $e^{\gamma} n \log \log n / 4$.

In Figure 2 we plot the extrapolation of this data. We do not present the corresponding semi-analytic expressions here, but note that while our subsequence data disagrees with [1] which uses a reduced $\mathbb{Z}_2 \times \mathbb{Z}_2$ Klein four-group symmetry, the total enumeration of invariant sublattices / inequivalent orbifolds is identical and the asymptotic data presented therein is thus consistent.

4.3 Orbifolds of dP_3

The orbifolds of the del Pezzo 3 surface can be represented by hexagonal toric diagrams with corresponding symmetry group D_6.

From [1] the cycle index for the dihedral group D_6 is given by (where $\varphi(d)$ is Euler's totient function):

$$Z(D_6) = \frac{1}{12} \sum_{d|6} \varphi(d) x_d^{6/d} + \frac{1}{4}(x_1^2 x_2^2 + x_2^3) \tag{37}$$

$$= \frac{1}{12}(x_1^6 + 2x_3^2 + 2x_6) + \frac{1}{4}x_1^2 x_2^2 + \frac{1}{3}x_2^3, \tag{38}$$

and so we obtain the corresponding relation for the number of sublattices of index n for the hexagonal lattice:

$$f^{\bigcirc} = \frac{1}{12}(f_{x_1^6}^{\bigcirc} + 4f_{x_2^3}^{\bigcirc} + 2f_{x_3^2}^{\bigcirc} + 2f_{x_6}^{\bigcirc} + 3f_{x_1^2 x_2^2}^{\bigcirc}). \tag{39}$$

Again we cannot take for granted that each individual term in the cycle index corresponds to a conjugacy class in D_6. Indeed, D_6 has in fact 6 conjugacy classes, not 5, with the last class coming from the fact that the 180-degree rotations form their own class. Therefore the cycle index is more appropriately written as:

$$f^{\bigcirc} = \frac{1}{12}(f_{x_1^6}^{\bigcirc} + 3f_{x_2^3}^{\bigcirc} + 2f_{x_3^2}^{\bigcirc} + 2f_{x_6}^{\bigcirc} + 3f_{x_1^2 x_2^2}^{\bigcirc} + f_{x_2^{3\prime}}^{\bigcirc}), \tag{40}$$

where the primed $x_2^{3\prime}$ corresponds to the 180-degree rotation.

Another way of stating this geometrically is as follows – D_6 is generated by elements x (rotation by $2\pi/6$) and y (reflection about the midpoint of an edge). The conjugacy classes that follow from this representation are:

$$\{1\}, \{x, x^5\}, \{x^3\}, \{y, yx^2, yx^4\}, \{yx, yx^3, yx^5\}.$$

Compare to the cycle index above, in particular noting the matching between the order of each conjugacy class and the coefficient of the relevant term in the cycle index.

An explicit description of the correspondence between the cycle index and the elements of D_6 in cycle notation is given in Table 3.

g	α_1	α_2	α_3	α_4	α_5	α_6	$c(\alpha_i)$	ζ
1	6	-	-	-	-	-	1	x_1^6
(12)(36)(45)	-	3	-	-	-	-	4	x_2^3
(14)(25)(36)	-	3	-	-	-	-	4	$x_2^{3\prime}$
(135)(246)	-	-	2	-	-	-	2	x_3^2
(13)(46)	2	2	-	-	-	-	3	$x_1^2 x_2^2$
(123456)	-	-	-	-	-	1	2	x_6

Table 3: Cycle index structure for the dihedral group D_6.

The conjugacy classes of D_6 correspond to the operations on the unit hexagon displayed in Figure 3.

There is no hexagon on a square lattice that respects D_6 symmetry exactly. Furthermore we cannot use the projection method as in the case of the triangular toric diagram. This is because the maximum interior angle formed by such a projection is $\pi/2$ whereas the hexagon demands $2\pi/3$ interior angle.
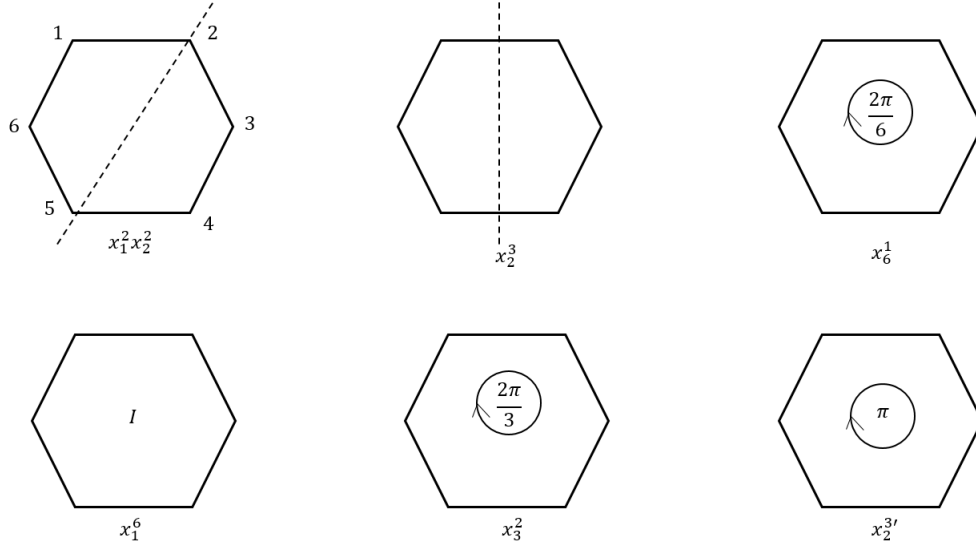
Figure 3: Representative operations of six conjugacy classes of D_6 operating on the hexagon. Compare to the representative elements of the permutation representation in Table 3.

However, we can linearly transform to a D_6-symmetric hexagon in the plane by rotating, scaling, and translating to the origin. Then a two-dimensional representation of D_6 suffices to check the algorithm.

The resulting numeric data for the dP_3 orbifold and symmetries of D_6 are displayed in Table 4.

n	1	2	3	4	5	6	7	8	9	10	11	12	13	14	15	16
$f^{\bigcirc}_{x_1^6}$	1	3	4	7	6	12	8	15	13	18	12	28	14	24	24	31
$f^{\bigcirc}_{x_1^2 x_2^2}$	1	1	2	3	2	2	2	5	3	2	2	6	2	2	4	7
$f^{\bigcirc}_{x_2^3}$	1	1	2	3	2	2	2	5	3	2	2	6	2	2	4	7
$f^{\bigcirc}_{x_2^{3'}}$	1	3	4	7	6	12	8	15	13	18	12	28	14	24	24	31
$f^{\bigcirc}_{x_3^2}$	1	0	1	1	0	0	2	0	1	0	0	1	2	0	0	1
$f^{\bigcirc}_{x_6^1}$	1	0	1	1	0	0	2	0	1	0	0	1	2	0	0	1
$f^{\bigcirc}$	1	1	2	3	2	3	3	5	4	4	3	8	4	5	6	9

Table 4: Number of sublattices of index n invariant under representative symmetries from each conjugacy class of D_6, for the orbifolds of dP_3.

Incredibly, we see that despite a completely different symmetry decomposition, it appears that the total number of equivalence classes of dP_3 orbifolds at each fixed n exactly agrees with the number of orbifolds of $\mathbb{C}^3$. The decomposition into each independent cycle is also intriguing, as each sequence is identical to one of the sequences for $f^{\triangle}$, appearing twice rather than once.

We do not reproduce analytic results for D_6 here since the semi-analytic expressions for the sequences are identical to that of S_3, as noted above.

4.4 Tetrahedral Toric Diagrams

The tetrahedron is the first of the Platonic solids that we will investigate. The symmetry group of the tetrahedron is given by S_4.

The cycle index for S_4 is

$$Z_{S_4} = \frac{1}{24} \left(x_1^4 + 6x_1^2 x_2 + 3x_2^2 + 8x_1 x_3 + 6x_4 \right), \tag{41}$$

corresponding to the conjugacy classes with representative elements:

$$\{(1), (12), (12)(34), (123), (1234).\} \tag{42}$$

To implement the S_4 action, we follow the following algorithm. First, we take as our unit tetrahedron the simplex with vertices at the origin and the three standard basis vectors of $\mathbb{R}^3$. The scaling procedure mentioned above was performed, expanding each Hermite normal form until a lattice point of each type was included. The scaling was then reversed and the Hermite normal form transformation inverted back to the unit tetrahedron, with the coordinates of each new lattice point recorded. This unit tetrahedron, however, is not regular and thus lacks most of the S_4 symmetry. Therefore, a bijection to a S_4-symmetric tetrahedron was constructed by mapping the points by the linear transformation A and translating by b, where A and b are given by:

$$A = \begin{pmatrix} 2 & 2 & 0 \\ 0 & -2 & -2 \\ 2 & 0 & 2 \end{pmatrix}, \qquad b = \begin{pmatrix} -1 \\ 1 \\ -1 \end{pmatrix}.$$

These maps take the unit tetrahedron described above to the S_4-symmetric tetrahedron with vertices at:

$$e_1 = (1, 1, 1), \tag{43}$$
$$e_2 = (1 - 1, -1), \tag{44}$$
$$e_3 = (-1, -1, 1), \tag{45}$$
$$e_4 = (-1, 1 - 1). \tag{46}$$

The action of S_4 was then implemented on this regular tetrahedron via the standard representation of S_4. This representation is three-dimensional and acts on the basis $\{e_1 - e_2, e_2 - e_3, e_3 - e_4\}$. Written in the standard basis of $\mathbb{R}^3$, representative elements from each conjugacy class can be written as:

$$(12) = \begin{pmatrix} 1 & 0 & 0 \\ 0 & 0 & -1 \\ 0 & -1 & 0 \end{pmatrix}, \qquad (123) = \begin{pmatrix} 0 & 0 & 1 \\ -1 & 0 & 0 \\ 0 & -1 & 0 \end{pmatrix}, \tag{47}$$

$$(12)(34) = \begin{pmatrix} 1 & 0 & 0 \\ 0 & -1 & 0 \\ 0 & 0 & -1 \end{pmatrix}, \qquad (1234) = \begin{pmatrix} 0 & 1 & 0 \\ -1 & 0 & 0 \\ 0 & 0 & -1 \end{pmatrix}. \tag{48}$$

The resulting data for S_4 is displayed in Table 5 out to $n = 16$, with corresponding extrapolation in Figure 5.
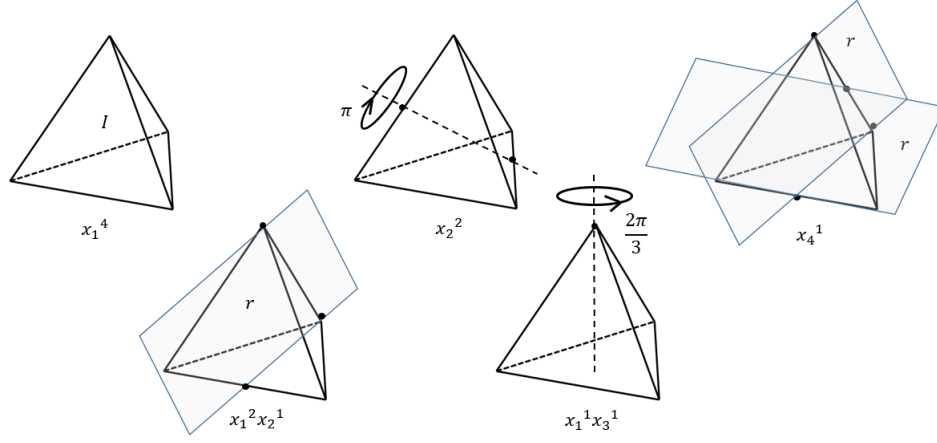
Figure 4: Symmetries of the tetrahedron, shown geometrically and labelled with their corresponding term in the cycle index.

n	1	2	3	4	5	6	7	8	9	10	11	12	13	14	15	16
$f_{x_1^4}^{\triangle}$	1	7	13	35	31	91	57	155	130	217	133	455	183	399	403	651
$f_{x_1^2 x_2}^{\triangle}$	1	3	5	11	7	15	9	31	18	21	13	55	15	27	35	75
$f_{x_2^2}^{\triangle}$	1	3	5	11	7	15	9	31	18	21	13	55	15	27	35	75
$f_{x_1 x_3}^{\triangle}$	1	1	1	2	1	1	3	2	4	1	1	2	3	3	1	3
$f_{x_4^1}^{\triangle}$	1	1	1	3	3	1	1	5	2	3	1	3	3	1	3	7
$f^{\triangle}$	1	2	3	7	5	10	7	20	14	18	11	41	15	28	31	58

Table 5: Number of sublattices of index n invariant under representative symmetries from each conjugacy class of S_4.

Semi-analytic results are reproduced below from [1]:

$$f_{x_1^4}^{\triangle} = u * N * N^2, \tag{49}$$

$$f_{x_1^2 x_2^1}^{\triangle} = \{1, -1, 0, 4\} * u * u * N, \tag{50}$$

$$f_{x_2^2}^{\triangle} = \{1, -1, 0, 4\} * u * u * N, \tag{51}$$

$$f_{x_1^1 x_3^1}^{\triangle} = \{1, 0, -1, 0, 0, 0, 0, 0, 3\} * u * u * \chi_{3,2}, \tag{52}$$

$$f_{x_4^1}^{\triangle} = \{1, -1, 0, 2\} * u * u * \chi_{4,2}. \tag{53}$$

We do not reproduce the corresponding generating functions and asymptotic data here.

4.5 Cubic Toric Diagrams

The construction for the cube is somewhat easier because the standard lattice basis of $\mathbb{Z}^3$ already possesses the desired $S_4 \times \mathbb{Z}_2$ symmetry. We need only translate the canonical unit cube to center it at the origin to find the regular cube for which we can implement the $S_4 \times \mathbb{Z}_2$ action.
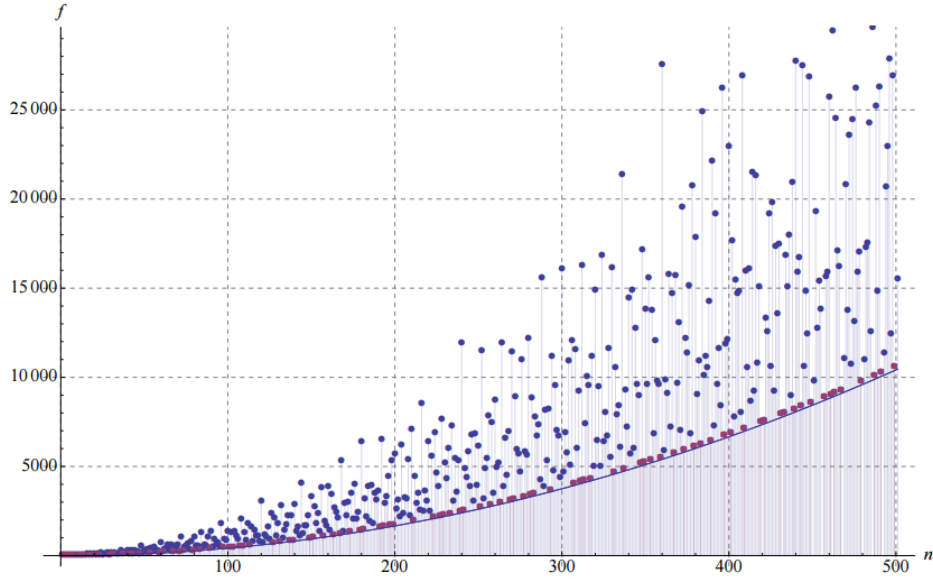
Figure 5: Scatter plot of the number of invariant sublattices of index n for the tetrahedral lattice. Primes are given in purple. The line corresponds to $n^2/24$.

The most intuitive way of representing the $S_4 \times \mathbb{Z}_2$ action on the cube is by permutation of the 4 space diagonals of the cube, with a $\mathbb{Z}_2$ toggle for possible inversion. One can rewrite the S_4 action in terms of rotations about different axes. Note that the direct product structure of the group tells us that the central inversion commutes with the S_4 action, since inversion commutes with rotation.

The conjugacy classes of S_4 have already been previously found. Since the inversions commute with the rotations, the conjugacy classes of $S_4 \times \mathbb{Z}_2$ are therefore two copies of the conjugacy classes of S_4; one with and one without inversion added. There are therefore ten total conjugacy classes, and we can write the cycle index as:

$$Z_{S_4 \times \mathbb{Z}_2} = \frac{1}{48} \left(x_1^{4+} + 6x_1^2 x_2^{1+} + 3x_2^{2+} + 8x_1^1 x_3^{1+} + 6x_4^{1+} + x_1^{4-} \right. \tag{54}$$

$$\left. + 6x_1^2 x_2^{1-} + 3x_2^{2-} + 8x_1^1 x_3^{1-} + 6x_4^{1-} \right), \tag{55}$$

where we have denoted the presence of the inversion by $+$ or $-$.

As previously stated, each term can be represented as a rotation of the cube about some axis, possibly combined with an inversion. The subscripts and superscripts used here in the cycle index refers to their geometric action on the space diagonals of the cube since this is the group that S_4 explicitly permutes. The geometric visualization of this action is shown in Figure 6.

Since inversion commutes through each rotation, the number of symmetric sublattices is the same whether or not one performs the inversion. We are thus free to restrict to the rotational subgroup of the icosahedral group, since the other half of the conjugacy classes will only duplicate the same numbers.

The resulting data is displayed in Table 6 out to $n = 18$. In Figure 7 the data is plotted using the closed forms described below out to $n = 500$.

There are five sequences we would like to be able to write in terms of Dirichlet convolutions. The first is given to us for free as it is just the number of sublattices in three dimensions, which is given in [1] as:
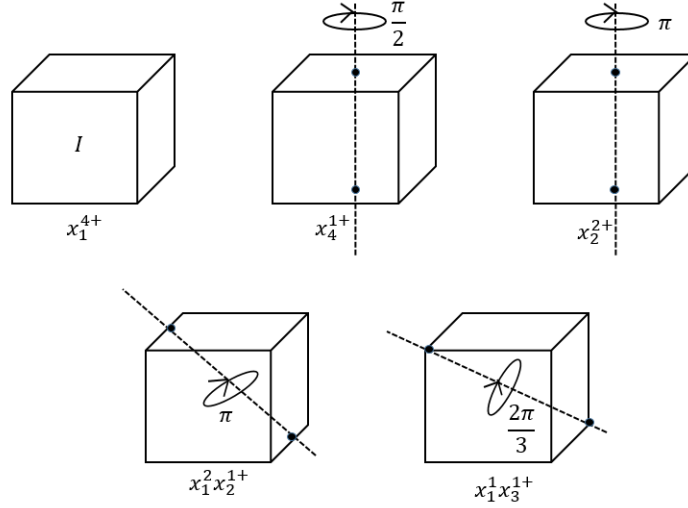
$$f_{x_1^{4+}}^{\square} = u * N * N^2. \tag{56}$$

15

Figure 6: Symmetries of the cube, shown geometrically and labelled with their corresponding term in the cycle index.

n	1	2	3	4	5	6	7	8	9	10	11	12	13	14	15	16	17	18
$f^{\square}_{x_1^{4+}}$	1	7	13	35	31	91	57	155	130	217	133	455	183	399	403	651	307	910
$f^{\square}_{x_1^2 x_2^{1+}}$	1	3	5	11	7	15	9	31	18	21	13	55	15	27	35	75	19	54
$f^{\square}_{x_2^{2+}}$	1	7	5	23	7	35	9	59	18	49	13	115	15	63	35	135	19	126
$f^{\square}_{x_1^1 x_3^{1+}}$	1	1	1	2	1	1	3	2	4	1	1	2	3	3	1	3	1	4
$f^{\square}_{x_4^{1+}}$	1	3	1	5	3	3	1	7	2	9	1	5	3	3	3	9	3	6
$f^{\square}$	1	3	3	9	5	13	7	24	14	23	11	49	15	33	31	66	21	70

Table 6: Number of sublattices of index n invariant under representative symmetries from each conjugacy class of $S_4 \times \mathbb{Z}_2$.

For the other monomial terms in the cycle index, we must make educated guesses for the closed-form sequences based on our limited data from explicitly counting. For $f^{\square}_{x_1^2 x_2^{1+}}$ and $f^{\square}_{x_1^1 x_3^{1+}}$, the work has already been done for us as the same subsequences appear in [1] as the subsequences corresponding to monomial terms in the cycle index of S_4 on the tetrahedral lattice. These are:

$$f^{\square}_{x_1^1 x_3^{1+}} = \{1, 0, -1, 0, 0, 0, 0, 0, 3\} * u * u * \chi_{3,2}, \tag{57}$$

$$f^{\square}_{x_1^2 x_2^{1+}} = \{1, -1, 0, 4\} * u * u * N. \tag{58}$$

The sequence $f^{\square}_{x_4^{1+}}$ we can write as the repeated convolution of a periodic sequence of length eight with the unit:

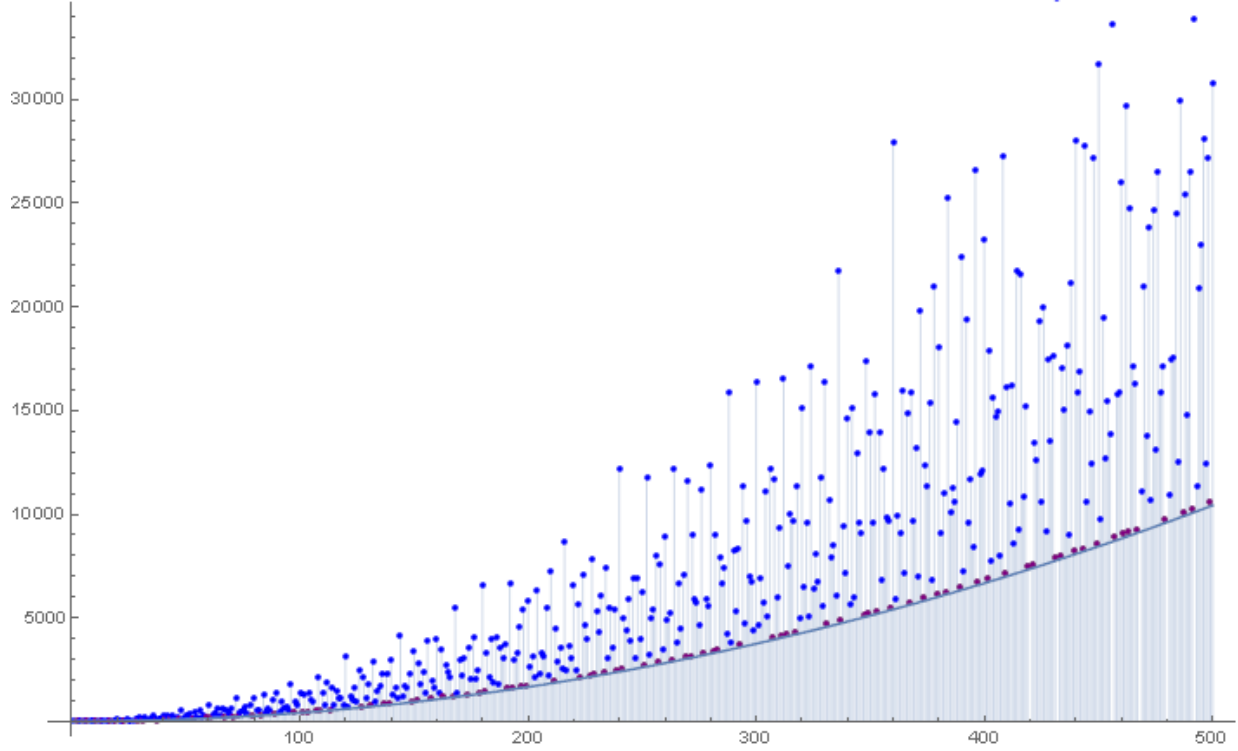$$f^{\square}_{x_4^{1+}} = \{1, 1, -1, 0, 1, -1, -1, 0, \ldots\} * u * u. \tag{59}$$

16

Figure 7: Scatter plot of the number of invariant sublattices of index n for the cubic lattice. Primes are given in purple. The line corresponds to $n^2/24$.

The repeated sequence $\{1, 1, -1, 0, 1, -1, -1, 0, \ldots\}$ can be decomposed as

$$\{1, 1, -1, 0, 1, -1, -1, 0, \ldots\} = \{1, 1\} * \chi_{4,2}, \tag{60}$$

so that we find:

$$f^{\square}_{x_4^{1+}} = \{1, 1\} * u * u * \chi_{4,2}. \tag{61}$$

Finally, the sequence $f^{\square}_{x_2^{2+}}$ can be written

$$f^{\square}_{x_2^{2+}} = \{1, 3\} * u * u * N. \tag{62}$$

Combining all of the results, we find that the sequence $f^{\square}$ can be written as

$$f^{\square} = \frac{1}{24} \left((\{8, 0, -8, 0, 0, 0, 0, 0, 24\} * \chi_{3,2} + \{6, 6\} * \chi_{4,2} + \{9, 3, 0, 24\} * N) * u * u + u * N * N^2 \right). \tag{63}$$

Let us first write out each term in the Dirichlet series, using the expressions from [1] wherever possible:

$$F^{\square}_{x_1^{4+}} = \zeta(s)\zeta(s-1)\zeta(s-2), \tag{64}$$

$$F^{\square}_{x_1^2 x_2^{1+}} = (1 - 2^{-s} + 2^{2-2s})\zeta(s)^2\zeta(s-1), \tag{65}$$

$$F^{\square}_{x_2^{2+}} = (1 + 3 \cdot 2^{-s})\zeta(s)^2\zeta(s-1), \tag{66}$$

$$F^{\square}_{x_1 x_3^{1+}} = (1 - 3^{-s} + 3^{1-2s})\zeta(s)^2 L(\chi_{3,2}, s), \tag{67}$$

$$F^{\square}_{x_4^{1+}} = (1 + 2^{-s})\zeta(s)^2 L(\chi_{4,2}, s), \tag{68}$$

17

So that the full Dirichlet series reads:

$$F^{\square}(s) = \frac{\zeta(s)}{24}\Big(\zeta(s-1)\zeta(s-2) + \big(6(1-2^{-s}+2^{2-2s}) + 3(1+3\cdot 2^{-s})\big)\zeta(s)\zeta(s-1) \tag{69}$$

$$+ \big(8(1+3^{-s}+3^{1-2s})L(\chi_{3,2},s) + 6(1+2^{-s})L(\chi_{4,2},s)\big)\zeta(s)\Big). \tag{70}$$

The Dirichlet series is holomorphic outside $s=3$, $s=2$, and $s=1$. The rightmost pole is thus $s=3$ and is of order 1, with residue $\frac{\zeta(2)\zeta(3)}{24}$. The asymptotic behavior of the partial sums of coefficients is thus:

$$\sum_{n=1}^{N} f^{\square}(n) \sim \frac{\zeta(2)\zeta(3)}{72}N^3. \tag{71}$$

Similarly, we can write down power series corresponding to each subsequence above:

$$G^{\square}_{x_1^{4+}} = \sum_{m,n,k=1}^{\infty} nm^2 t^{mnk}, \tag{72}$$

$$G^{\square}_{x_1^2 x_2^{1+}} = \sum_{m,n,k=1}^{\infty} m(t^{mnk} - t^{2mnk} + 4t^{4mnk}), \tag{73}$$

$$G^{\square}_{x_2^{2+}} = \sum_{m,n,k=1}^{\infty} m(t^{mnk} + 3t^{2mnk}), \tag{74}$$

$$G^{\square}_{x_1^1 x_3^{1+}} = \frac{1}{2}\sum_{k=1}^{\infty}\sum_{m,n=-\infty}^{\infty} \big(t^{k(n^2+mn+7m^2)} - 1\big), \tag{75}$$

$$G^{\square}_{x_4^{1+}} = \sum_{k,n=1}^{\infty} \frac{(3+(-1)^n)t^{kn}}{2(1+t^{2kn})} = \frac{1}{2}\sum_{k,n,m=1}^{\infty} (-1)^{2kmn}(3+(-1)^n)t^{kn(2m+1)}. \tag{76}$$

where in the last sum above we have written it as a formal power series instead of a rational series using geometric series expansion. In these expressions, the coefficient of t^j is the jth coefficient of each corresponding subsequence, and all $j \leq 0$ are to be disregarded (Note: the only sequence for which this matters was taken from [1]; I believe there is an erroneous constant factor in that paper).

4.6 Dodecahedral Toric Diagrams

The symmetry group of the dodecahedron is is given by $A_5 \times \mathbb{Z}_2$, the icosahedral group, of order 120. The A_5 factor corresponds to the subgroup of rotational symmetries of the dodecahedron, with the $\mathbb{Z}_2$ giving inversion of the dodecahedron via the operation $\vec{x} \to -\vec{x}$. The A_5 action can be realized explicitly as the permutations of the five unique tetrahedra that inscribe in the dodecahedron by partitioning vertices. Since the inversion commutes with all rotations it is sufficient to consider the A_5 rotational subgroup in the cycle index. There are ten total conjugacy classes, but only five when restricted to the rotational subgroup. These can be described as:

- Identity

- 12 rotations by multiples of $2\pi/5$ and not $4\pi/5$ about the center of a face

- 12 rotations by multiples $4\pi/5$ about the center of a face
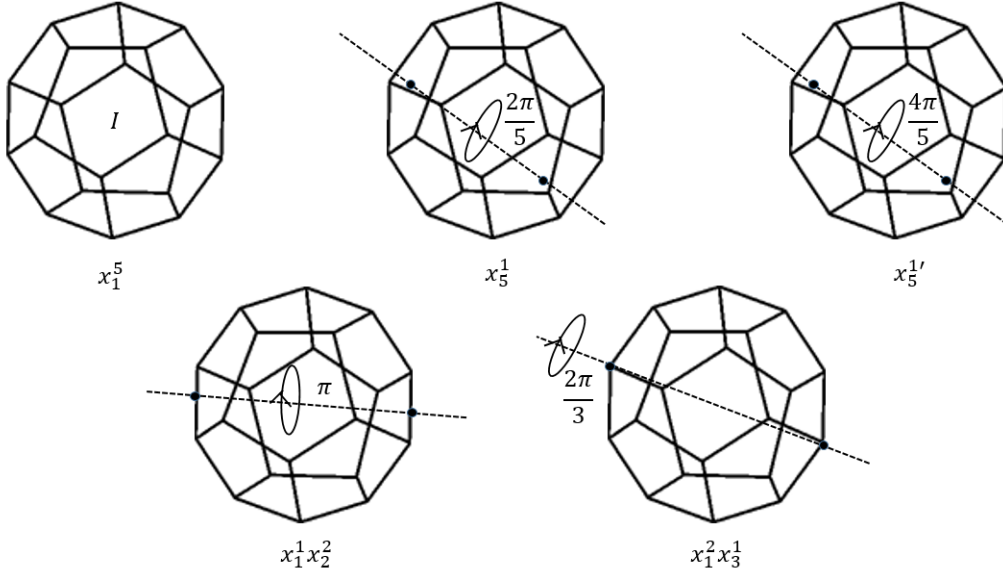
- 20 rotations by multiples of $2\pi/3$ about a vertex

Figure 8: Rotational symmetries of the dodecahedron, shown geometrically and labelled with their corresponding term in the cycle index.

- 15 rotations by π about the center of an edge

The geometric visualization of the A_5 action is shown in Figure 8.

We can thus write the cycle index as

$$Z_{A_5 \times \mathbb{Z}_2} = \frac{1}{60}\left(x_1^5 + 12x_5^1 + 12x_5^{1'} + 20x + 15x \right). \tag{77}$$

The distinction between x_5^1 and $x_5^{1'}$ comes from the splitting of the five-cycle conjugacy class in A_5 corresponding to the two distinct five-fold rotational symmetries above.

The case of the dodecahedron is highly nontrivial because the vertices of the dodecahedron do not live on a cubic lattice in three dimensions even after linear transformation. One requires a lattice where the unit has $A_5 \times \mathbb{Z}_2$ symmetry, scaling the unit does not break this symmetry, and transforming the unit by a HNF does not move off the lattice. The existence of such a lattice is prevented by the crystallographic restriction on space groups in three dimensions. Namely, there exists no three-dimensional lattice with five-fold symmetry. Furthermore, the highest order symmetry group permissible for a lattice in $\mathbb{R}^3$ is of order 48, which is too small to accomodate the order 60 symmetries of A_5.

One potential alternative method for the dodecahedron is to embed into one higher dimension, where five-fold symmetry is permissible, and find the appropriate projection to the three-dimensional lattice to count symmetries. However, such an approach is computationally expensive since many of the algorithms involved are asymptotically factorial or worse in the number of dimensions. Furthermore it is not clear how to actually implement such a projection.

An approach that may bear fruitful results rests on the following remarkable observation: there exists a startling correspondence between the symmetry groups of Platonic solids and projective linear groups over finite fields. Namely, we have the isomorphisms:

$$S_3 \simeq \mathrm{PGL}(2, \mathbb{F}_2), \tag{78}$$
$$S_4 \simeq \mathrm{PGL}(2, \mathbb{F}_3), \tag{79}$$
$$A_5 \simeq \mathrm{PGL}(2, \mathbb{F}_4). \tag{80}$$

19

This suggests the possibility that the invariant sublattice question can be rephrased in terms of questions of projective geometry. This observation has not yet produced any results but seems promising for future study.

5   Acknowledgments

References

[1] Hanany, Amihay; Orlando, Domenico, and Susanne Reffert. "Sublattice Counting and Orbifolds." http://arxiv.org/pdf/1002.2981v1.pdf.

[2] Hanany, Amihay and Rak-Kyeong Seong. "Symmetries of Abelian Orbifolds." http://arxiv.org/abs/1009.3017.

[3] Davey, John; Hanany, Amihay, and Rak-Kyeong Seong. "An Introduction to Counting Orbifolds." http://arxiv.org/abs/1102.0015.

[4] Davey, John; Hanany, Amihay, and Rak-Kyeong Seong. "Counting Orbifolds." http://arxiv.org/pdf/1002.3609.pdf.

[5] Feng, Bo; Franco, Sebastian; Hanany, Amihay, and Yang-Hui He. "Unhiggsing the del Pezzo." http://arxiv.org/abs/hep-th/0209228.

[6] Hanany, Amihay and Yang-Hui He. "Chern-Simons: Fano and Calabi-Yau." http://arxiv.org/abs/0904.1847.

[7] Feng, Bo; Franco, Sebastián; Hanany, Amihay, and Yang-Hui He. "Symmetries of Toric Duality." http://xxx.lanl.gov/pdf/hep-th/0205144v3.pdf.

[8] McKay, John "Graphs, singularities and finite groups", Proc. Symp. Pure Math. 37, 183 (1980).

[9] Franco, Sebastian; Hanany, Amihay; Kennaway, Kristian D.; Vegh, David, and Brian Wecht. "Brane Dimers and Quiver Gauge Theories." http://arxiv.org/abs/hep-th/0504110.